Cellular/Molecular

Ca^{2+}-Dependent, Phospholipid-Binding Residues of Synaptotagmin Are Critical for Excitation–Secretion Coupling *In Vivo*

Brie E. Paddock,[1] Amelia R. Striegel,[1] Enfu Hui,[2] Edwin R. Chapman,[2] and Noreen E. Reist[1]

[1]Molecular, Cellular, and Integrative Neuroscience Program, Department of Biomedical Sciences, Colorado State University, Fort Collins, Colorado 80523, and [2]Howard Hughes Medical Institute and Department of Physiology, University of Wisconsin, Madison, Wisconsin 53706

Synaptotagmin I is the Ca^{2+} sensor for fast, synchronous release of neurotransmitter; however, the molecular interactions that couple Ca^{2+} binding to membrane fusion remain unclear. The structure of synaptotagmin is dominated by two C_2 domains that interact with negatively charged membranes after binding Ca^{2+}. *In vitro* work has implicated a conserved basic residue at the tip of loop 3 of the Ca^{2+}-binding pocket in both C_2 domains in coordinating this electrostatic interaction with anionic membranes. Although results from cultured cells suggest that the basic residue of the C_2A domain is functionally significant, such studies provide contradictory results regarding the importance of the C_2B basic residue during vesicle fusion. To directly test the functional significance of each of these residues at an intact synapse *in vivo*, we neutralized either the C_2A or the C_2B basic residue and assessed synaptic transmission at the *Drosophila* neuromuscular junction. The conserved basic residues at the tip of the Ca^{2+}-binding pocket of both the C_2A and C_2B domains mediate Ca^{2+}-dependent interactions with anionic membranes and are required for efficient evoked transmitter release. Our results directly support the hypothesis that the interactions between synaptotagmin and the presynaptic membrane, which are mediated by the basic residues at the tip of both the C_2A and C_2B Ca^{2+}-binding pockets, are critical for coupling Ca^{2+} influx with vesicle fusion during synaptic transmission *in vivo*. Our model for synaptotagmin's direct role in coupling Ca^{2+} binding to vesicle fusion incorporates this finding with results from multiple *in vitro* and *in vivo* studies.

Key words: **synaptotagmin; synaptic vesicle fusion; anionic phospholipid interactions; site-directed mutagenesis; electrophysiology; calcium dependence; Western analysis; immunohistochemistry; *Drosophila***

Introduction

The synaptic vesicle protein, synaptotagmin, functions as the Ca^{2+} sensor for synchronous neurotransmitter release. Synaptotagmin contains two C_2 domains, C_2A and C_2B, that coordinate Ca^{2+} ions. Whereas Ca^{2+} binding by the C_2B domain is essential for synchronous transmitter release, Ca^{2+} binding by C_2A plays only a modest role (Fernández-Chacón et al., 2002; Mackler et al., 2002; Robinson et al., 2002). Synaptotagmin's C_2 domains interact with anionic phospholipids in a Ca^{2+}-dependent manner *in vitro* (Perin et al., 1990; Earles et al., 2001; Fernández-Chacón et al., 2001; Bai et al., 2002), and deficits in Ca^{2+}-triggered fusion in several synaptotagmin mutants parallel the decrease in Ca^{2+}-dependent phospholipid binding (Fernández-Chacón et al., 2001; Mackler et al., 2002; Sørensen et al., 2003; Wang et al., 2003; Nishiki and Augustine, 2004; Li et al., 2006). Thus, a Ca^{2+}-dependent interaction between synaptotagmin and phospholipids is postulated to be critical in mediating Ca^{2+}-triggered vesicle fusion.

Specific residues within synaptotagmin are required for Ca^{2+}-dependent phospholipid binding *in vitro*. At the tip of the Ca^{2+}-binding loops of each C_2 domain, there is a conserved basic residue (Fig. 1, ⊕) that is thought to mediate an electrostatic interaction between synaptotagmin and the anionic presynaptic membrane (Chae et al., 1998; Fernández-Chacón et al., 2001; Wang et al., 2003). This interaction may contribute to the electrostatic switch that drives vesicle fusion after Ca^{2+} influx (Davletov et al., 1998; Ubach et al., 1998). In C_2A, this basic residue is likely functionally significant, because it is necessary for efficient Ca^{2+}-triggered vesicle fusion in a variety of cultured cell types (Fernández-Chacón et al., 2001; Sørensen et al., 2003; Wang et al., 2003). The functional significance of this basic residue in C_2B, however, is controversial, because studies from cultured cells provide contradictory results (Wang et al., 2003; Li et al., 2006). In addition, cultured cells do not necessarily reproduce the exact behavior of intact synapses (Banker and Goslin, 1998), so it is critical to test each of these residues for function *in vivo*.

Because (1) multiple residues located at the tip of the Ca^{2+}-binding pockets, including these basic residues, in both the C_2A

Received May 15, 2007; revised June 3, 2008; accepted June 5, 2008.

This work was supported by grants from American Heart Association (0440168N), March of Dimes, National Institutes of Health (NS-045865, GM 56827, and MH 61876), and National Science Foundation (9982862). E.R.C. is an Investigator of the Howard Hughes Medical Institute. We thank Laurie Biela for her technical assistance, Dr. Thomas Südhof for the mammalian synaptotagmin GST-C_2AB constructs, and Dr. Sandra Bajjalieh for providing the GST-KG vector.

Correspondence should be addressed to Dr. Noreen E. Reist, Molecular, Cellular, and Integrative Neuroscience Program, Department of Biomedical Sciences, Colorado State University, Fort Collins, CO 80523-1617. E-mail: reist@lamar.colostate.edu.

DOI:10.1523/JNEUROSCI.0197-08.2008

 0270-6474/08/287458-09$15.00/0

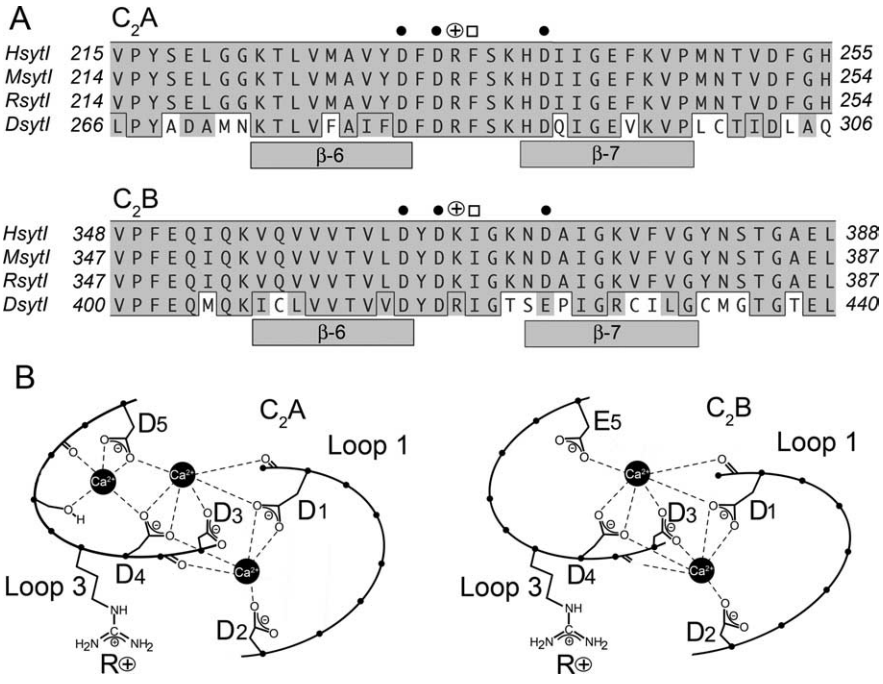

Figure 1. Both the C_2A and C_2B domains of synaptotagmin I have a conserved basic residue at the tip of the Ca^{2+}-binding pocket. ***A***, Alignment of synaptotagmin I from human, rat, mouse, and *Drosophila*. Bars indicate β-sheets, ⊕ indicates the conserved basic residues, dots indicate Ca^{2+}-binding residues, and open boxes indicate conserved hydrophobic residues. Within the alignment, conserved residues are shown in gray, and identical residues are boxed. ***B***, Schematic representation of loops 1 and 3, which form the Ca^{2+}-binding pockets of both C_2 domains [adapted with permission from Fernandez et al. (2001), their Fig. 6, using the *Drosophila* sequence to show the conserved basic residues (⊕) examined in this study].

and C_2B domains are critical for Ca^{2+}-dependent phospholipid interactions (Chae et al., 1998; Chapman and Davis, 1998; Davis et al., 1999; Fernández-Chacón et al., 2001; Bai et al., 2002; Frazier et al., 2003; Wang et al., 2003; Araç et al., 2006) (but see Li et al., 2006) and (2) multiple fusion assays implicate these tip residues in Ca^{2+}-triggered fusion (Fernández-Chacón et al., 2001; Sørensen et al., 2003; Wang et al., 2003; Rhee et al., 2005; Martens et al., 2007), we directly tested the functional significance of each of these basic residues at an intact synapse by individually neutralizing them and measuring evoked release at the *Drosophila* neuromuscular junction. Here, we demonstrate that the conserved basic residues at the tip of the C_2A and C_2B Ca^{2+}-binding pockets each mediate interactions with anionic phospholipids *in vitro* and are each critical for synaptotagmin function *in vivo*.

Materials and Methods

Site-directed mutagenesis. To neutralize the positive charge without disrupting the structure of the C_2 domain (Fernández-Chacón et al., 2001), arginine residues 285 and 419 (Fig. 1, ⊕) of *Drosophila* synaptotagmin I (syt) were mutated to glutamines using PCR. To mutate arginine 285, a specifically mutated oligonucleotide (CGAGAACTGATCGAAGTCGAAAATGGC) was paired with a wild-type (WT) oligonucleotide that flanked a unique *Sty*I site. The PCR product was gel purified and used as a macroprimer in a second round of PCR with a wild-type oligonucleotide that flanked a unique *Eco*RV site. This second-round, mutant PCR product was then subcloned into an otherwise wild-type *Drosophila syt* cDNA construct in pBluescript II (Mackler and Reist, 2001). To mutate arginine 419, a specifically mutated oligonucleotide (TGCAGCGGCCGATGGGTTCGGAGGTGCCAATCTGATCGTAGTCCACGACGGTCACAACG) containing a unique *Eag*I site was paired with a wild-type oligonucleotide that flanked a unique *Eco*RV site. That mutant PCR product was then gel purified and subcloned into the *Drosophila syt* cDNA construct in pBluescript mentioned above. DNA sequencing confirmed that either R285Q or R419Q was the only mutation harbored in the entire region generated by PCR. Each mutant *syt* cDNA was subcloned into a pUAST vector to place the mutant *syt* gene under the control of the UAS promoter (Brand and Perrimon, 1993).

Generation of mutant transgenic lines. Drosophila embryos were transfected with the mutant pUAST plasmids as described previously (Mackler and Reist, 2001). At least two lines carrying separate insertions of the mutant *syt* transgenes were isolated for each genotype. Expression of each transgene was localized to the nervous system using the elav promoter to drive Gal4, and the Gal4/UAS system was used to amplify expression levels (Brand and Perrimon, 1993; Yao and White, 1994). Standard genetic techniques were used to cross the transgenes into the syt^{null} background to express the transgene in the absence of endogenous synaptotagmin I for all experiments. The genotypes of the mutant lines were *yw;* syt^{AD4} *elav GAL4/*syt^{AD4}*;* $P[UAS\ syt^{A\text{-}R285Q}]/+$, and *yw;* syt^{AD4} *elav GAL4/*syt^{AD4}*;* $P[UAS\ syt^{B\text{-}R419Q}]/+$, which are written as $P[syt^{A\text{-}RQ}]$ and $P[syt^{B\text{-}RQ}]$, respectively, in the text. The genotype of the control was *yw;* syt^{AD4} *elav GAL4/*syt^{AD4}*;* $P[UAS\ syt^{wild\text{-}type}]/+$, which is written as $P[syt^{WT}]$ in the text.

Electrophysiology. Evoked and spontaneous excitatory junction potentials (EJPs) were recorded from muscle 6 of segments 3 and 4 of third instars in HL3 saline [5 mM KCl, 1.5 mM $CaCl_2$, 70 mM NaCl, 20 mM $MgCl_2$, 10 mM $NaCHO_3$, 5 mM HEPES, 115 mM sucrose, and 5 mM trehalose (Stewart et al., 1994)] as described previously (Loewen et al., 2001). Briefly, third-instar larvae were dissected in Ca^{2+}-free HL3 to expose the body wall musculature. After changing to HL3 saline containing 1.5 mM Ca^{2+}, muscle 6 was impaled with a recording electrode having a resistance between 10 and 40 MΩ. Evoked EJPs were generated by stimulating segmental nerves with a suction electrode filled with HL3. The Ca^{2+} dependence curve was generated by evoking EJPs in external Ca^{2+} concentrations ranging from 0.6 to 5.0 mM. Muscles were impaled in 1.5 mM Ca^{2+} HL3, and recordings in several different Ca^{2+} concentrations were obtained from each muscle fiber. The trehalose was varied between 0.5 and 5.0 mM, although this had no effect on evoked release (data not shown). The predicted maximal response was calculated by fitting the Hill equation to the mean response at each extracellular Ca^{2+} concentration (Kaledіagraph). The Ca^{2+} cooperativity coefficient was estimated from the slope of a double-log plot of EJP amplitude versus Ca^{2+} concentration (Kaledіagraph). All events were collected using an AxoClamp 2B (Molecular Devices) and digitized using a MacLab4s analog-to-digital converter (ADInstruments). Spontaneous events were recorded in Chart Software, and evoked events were recorded in Scope software (ADInstruments). Spontaneous fusion events were identified manually, blind to genotype.

Immunolabeling. For immunolabeling of the neuromuscular junction, third instars of the indicated genotypes were dissected in Ca^{2+}-free HL3 saline to expose their body wall muscles and fixed in 4% paraformaldehyde in PBS. This whole-mount preparation was incubated overnight in anti-synaptotagmin antibody [Dsyt-CL1 (Mackler et al., 2002)], diluted 1:1000 in PBST-NGS [PBS with 0.1% Triton, 1% BSA, and 1% normal goat serum (NGS from Jackson ImmunoResearch)], washed in PBST for 30–60 min, incubated in Alexa Fluor 488 goat-anti-rabbit antibody (Invitrogen) diluted 1:5000 in PBST-NGS for 1 h, washed in PBST for 1–2 h, mounted in Citifluor (Ted Pella), and then visualized on a Zeiss LSM 510Meta confocal microscope equipped with an argon laser (Zeiss Microimaging). Emissions were collected using a bandpass 505–530 emission filter at 40× with a pinhole set for 1 Airy unit.

Immunoblotting. Similar levels of transgene expression were verified by Western blot analysis. The nervous system of a single third instar of the

indicated genotype was homogenized in protein loading buffer (Bio-Rad). Proteins were separated via SDS-PAGE and transferred to a polyvinylidene difluoride membrane as described previously (Mackler and Reist, 2001). All antibodies were diluted in PBS containing 0.05% Tween and 10% NGS. Blots were probed with Dsyt-CL1 diluted between 1:1250 and 1:5000, and an anti-actin antibody (MAB 1501; Millipore Bioscience Research Reagents), diluted between 1:20,000 and 1:80,000. Actin levels were used to normalize for equal protein loading. These antibodies were visualized with HRP-tagged donkey anti-rabbit IgG, diluted 1:10,000 to 1:20,000, and HRP-tagged donkey anti-mouse IgG, diluted 1:2500 to 1:40,000 (Jackson ImmunoResearch). The HRP-tagged antibodies were detected using a Supersignal West Dura Extended Duration Substrate kit (Pierce) in an Epichemi3 Darkroom (UVP). The synaptotagmin:actin signal ratio was determined for each CNS, then normalized to the mean synaptotagmin:actin ratio of the $P[syt^{WT}]$ lanes on each blot to allow comparison of signal between multiple blots.

C_2AB–phospholipid binding. cDNA encoding the cytoplasmic domain of *Drosophila* synaptotagmin (C_2AB, residues 191–474) was generated by PCR using primers AGCAGAGAATTCAGAAGCTGGGGCGCC and CCGCCGAAGCTTTTACTTCATGTTCTT. WT, C_2A mutant (A-R285Q), and C_2B mutant (B-R419Q) C_2AB constructs were subcloned into the expression vector, pGEX-KG (kindly provided by Dr. Sandra Bajjalieh, University of Washington, Seattle, WA). Mammalian cDNA encoding WT, C_2A mutant (A-R233Q), and C_2B mutant (B-K366Q) C_2AB in pGEX-KG (Li et al., 2006) was kindly provided by Dr. Thomas C. Südhof (UT Southwestern Medical Center, Dallas, TX). The C_2AB domains were expressed as GST fusion proteins and purified using glutathione-Sepharose beads [GE Healthcare (Chapman et al., 1995)]. Recombinant synaptotagmin harbors tightly bound nucleic acid contaminants that may affect its properties (Ubach et al., 2001). These contaminants were removed by DNase/RNase and high-salt washes as described previously (Bai et al., 2004). Synthetic 1,2-dioleoyl-sn-glycero-3-phospho-L-serine [phosphatidylserine (PS)], 1,2-dioleoyl-sn-glycero-3-phosphocholine [phosphatidylcholine (PC)], and *N*-(lissamine rhodamine B sulfonyl)-1,2-dipalmitoyl-sn-glycero-3-phosphoethanolamine were purchased from Avanti Polar Lipids. A phospholipid mixture containing 15% negatively charged phospholipid was chosen to approximate the amount of negatively charged phospholipids found in neuronal membranes (Takamori et al., 2006). This mixture [15% PS + 84% PC + 1% *N*-(lissamine rhodamine B sulfonyl)-1,2-dipalmitoyl-sn-glycero-3-phosphoethanolamine] was dried under a stream of nitrogen and suspended in HEPES-buffered saline (50 mM HEPES/150 mM NaCl, pH 7.4). Large (100 nm) unilamellar liposomes were prepared using an extruder from Avanti Polar Lipids, as described previously (Davis et al., 1999). Rhodamine-labeled liposome-binding assays were performed as described previously (Hui et al., 2005) in 150 μl of HEPES-buffered saline (50 mM HEPES/150 mM NaCl, pH 7.4) using 6 μg of immobilized protein and 22 nM liposomes per data point. Bound liposomes were eluted with HEPES-buffered saline containing 1% Triton X-100. The solubilized lipids were collected, and binding was quantified by measuring the emission fluorescence intensity of rhodamine at 580 nm. To determine the apparent Ca^{2+} affinity for WT and mutant C_2AB, we assayed for PS/PC binding as a function of the indicated Ca^{2+} concentrations. Free Ca^{2+} concentration was calculated by using WEBMAXC STANDARD software developed by Stanford University (http://www.stanford.edu/~cpatton/webmaxc/webmaxcS.htm). Data were plotted and fitted with sigmoidal dose–response curves (variable slope) using PRISM 5.0 software (GraphPad). In all experiments, error bars represent the SD from at least three independent determinations.

Results

The conserved basic residues at the tips of synaptotagmin's C_2A and C_2B Ca^{2+}-binding pockets are both required for efficient synaptic transmission

A highly conserved basic residue is present in loop 3 of the Ca^{2+}-binding pocket in both the C_2A and C_2B domains of synaptotagmin I (Fig. 1, ⊕). To examine the role of these residues during synaptic transmission at an intact synapse, we separately mutated the conserved basic residue in each C_2 domain to a glutamine and assessed evoked release at the *Drosophila* neuromuscular junction. We will denote the mutation of these residues as $syt^{A\text{-}RQ}$ and $syt^{B\text{-}RQ}$. All experiments were performed on third instars expressing the indicated form of synaptotagmin from a transgene in the absence of endogenous synaptotagmin I. To indicate their transgenic origin, we will refer to the C_2A mutants as $P[syt^{A\text{-}RQ}]$, the C_2B mutants as $P[syt^{B\text{-}RQ}]$, and the transgenic controls as $P[syt^{WT}]$. Finally, because the random insertion of a transgene could potentially disrupt another functionally important gene, two independent insertions of each mutant transgene were examined to ensure that any deficits found resulted from the mutation rather than the insertion site.

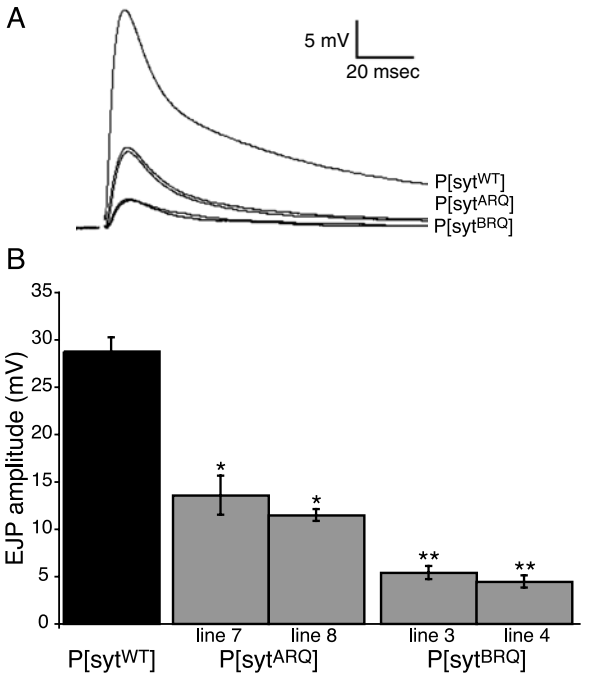

Figure 2. Evoked release is reduced in phospholipid-binding mutants of both C_2 domains. ***A***, Representative traces recorded from larval muscle fiber 6. Each trace represents the mean of 30 consecutive sweeps from the same muscle fiber. ***B***, Compared with $P[syt^{WT}]$, the mean EJP amplitude of all $P[syt^{RQ}]$ lines was significantly decreased (*, **$p < 0.0001$, 1-way ANOVA; $P[syt^{WT}]$, $n = 16$; $P[syt^{A\text{-}RQ}]$ line 7, $n = 12$; $P[syt^{A\text{-}RQ}]$ line 8, $n = 14$; $P[syt^{B\text{-}RQ}]$ line 3, $n = 16$; $P[syt^{B\text{-}RQ}]$ line 4, $n = 13$). Additionally, the evoked responses of the $P[syt^{B\text{-}RQ}]$ lines were significantly lower than those of the $P[syt^{A\text{-}RQ}]$ lines (*, **$p < 0.01$), but no differences were found between $P[syt^{A\text{-}RQ}]$ lines 7 and 8, or between $P[syt^{B\text{-}RQ}]$ lines 3 and 4 ($p > 0.2$).

Evoked EJPs and spontaneous miniature excitatory junction potentials (mEJPs) were recorded from larval neuromuscular junctions in HL3 saline containing 1.5 mM Ca^{2+}. Mutation of either of the conserved basic residues that mediate synaptotagmin's electrostatic interaction with anionic phospholipids decreased the evoked response (Fig. 2). The mutation within the C_2A domain reduced evoked release by ~50% compared with the transgenic wild-type control. Evoked release in $P[syt^{A\text{-}RQ}]$ was 13.6 ± 2.1 mV (line 7) or 11.5 ± 0.6 mV (line 8) compared with 27.4 ± 1.5 mV in $P[syt^{WT}]$ (Fig. 2*B*, asterisks) ($p < 0.0001$). This decrease is similar to the result observed in cultured cells from mice and rats harboring a homologous mutation (Fernández-Chacón et al., 2001; Sørensen et al., 2003; Wang et al., 2003; Han et al., 2004). The mutation within the C_2B domain reduced evoked release by ~80% compared with the transgenic control. Evoked release in the $P[syt^{B\text{-}RQ}]$ mutants was 5.4 ± 0.7 mV (line 3) or 4.4 ± 0.7 mV (line 4), compared with 27.4 ± 1.5 mV in

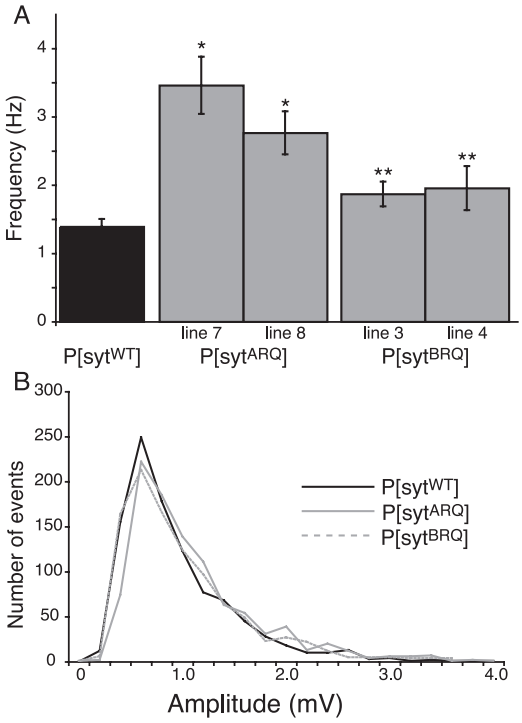

Figure 3. mEJP frequency is increased in phospholipid-binding mutants of both C_2 domains. ***A***, Mean mEJP frequencies of each mutant and the transgenic control. $P[syt^{WT}]$, $n = 55$ fibers; $P[syt^{A\text{-}RQ}]$ line 7, $n = 7$ fibers; $P[syt^{A\text{-}RQ}]$ line 8, $n = 17$ fibers; $P[syt^{B\text{-}RQ}]$ line 3, $n = 27$ fibers; $P[syt^{B\text{-}RQ}]$ line 4, $n = 12$ fibers. Compared with $P[syt^{WT}]$, all genotypes had an increased mEJP frequency ($p < 0.05$). No significant difference was detected between $P[syt^{A\text{-}RQ}]$ and $P[syt^{B\text{-}RQ}]$ ($p > 0.05$), between $P[syt^{A\text{-}RQ}]$ lines 7 and 8 ($p > 0.1$), or between $P[syt^{B\text{-}RQ}]$ lines 3 and 4 ($p > 0.1$). $^*p < 0.0001$, $^{**}p < 0.05$, compared with $P[syt^{WT}]$. ***B***, Frequency distribution curves of mEJP amplitudes calculated from 1000 individual events per transgenic line in 0.2 mV bins. $P[syt^{WT}]$, $P[syt^{A\text{-}RQ}]$ line 8, and $P[syt^{B\text{-}RQ}]$ line 3 are shown.

$P[syt^{WT}]$ (Fig. 2*B*, double asterisks) ($p < 0.0001$). This decrease is consistent with results from cultured rat neuroendocrine cells, PC12 cells (Wang et al., 2003), but in direct contrast to the results from cultured mouse neurons, hippocampal autapses (Li et al., 2006). The level of evoked release remaining in the $P[syt^{B\text{-}RQ}]$ mutants is significantly less than that in the $P[syt^{A\text{-}RQ}]$ mutants (Fig. 2*B*, asterisks vs double asterisks) ($p < 0.01$). No difference in mean EJP amplitude was found between the insertions of a given genotype for either $P[syt^{A\text{-}RQ}]$ or $P[syt^{B\text{-}RQ}]$ ($p > 0.2$). Thus, the reduction in evoked release results from the specific synaptotagmin mutations and not from insertion of the transgene disrupting an unspecified gene.

Mutation of either of the conserved basic residues increases the rate of spontaneous release at third-instar neuromuscular junctions (Fig. 3*A*). The mutation within the C_2A domain at least doubled the rate of mEJPs, with a frequency of 3.5 ± 0.4 Hz (line 7) or 2.8 ± 0.3 Hz (line 8) in $P[syt^{A\text{-}RQ}]$ compared with 1.4 ± 0.1 Hz in $P[syt^{WT}]$ (Fig. 3*A*, asterisks) ($p < 0.0001$). The mutation within the C_2B domain increased the rate of mEJPs by ~40%, to 1.9 ± 0.2 Hz (line 3) or 2.0 ± 0.3 Hz (line 4) compared with 1.4 ± 0.1 Hz for $P[syt^{WT}]$ (Fig. 3*A*, double asterisks) ($p < 0.05$). Although the trend toward a less severe increase in mEJP frequency in the C_2B mutants suggests that these mutants may maintain more of a vesicle-clamping function, the frequency of mEJPs in the $P[syt^{A\text{-}RQ}]$ and $P[syt^{B\text{-}RQ}]$ mutants was not significantly different ($p > 0.05$, single asterisks vs double asterisks, one-way ANOVA). No difference in mEJP frequency was found between independent insertions of the synaptotagmin gene for $P[syt^{A\text{-}RQ}]$ or $P[syt^{B\text{-}RQ}]$ (Fig. 3*A*) ($p > 0.2$). The amplitude of mEJPs was unchanged in the mutants ($P[syt^{WT}]$, 1.10 ± 0.03 mV; $P[syt^{A\text{-}RQ}]$ line 7, 1.00 ± 0.08 mV; $P[syt^{A\text{-}RQ}]$ line 8, 1.24 ± 0.06 mV; $P[syt^{B\text{-}RQ}]$ line 3, 1.09 ± 0.06 mV; $P[syt^{B\text{-}RQ}]$ line 4, 1.10 ± 0.07 mV; $p > 0.1$, one-way ANOVA). In addition, we compared the frequency of quantal amplitudes for each mutant line (Fig. 3*B*) ($P[syt^{WT}]$, $P[syt^{A\text{-}RQ}]$ line 8, and $P[syt^{B\text{-}RQ}]$ line 3 shown). The constant mEJP amplitude indicates that neither the C_2A nor the C_2B mutation perturbs synaptic vesicle filling or the postsynaptic machinery and is consistent with previous studies of spontaneous release characteristics in $syt^{A\text{-}RQ}$ mutants (Sørensen et al., 2003).

The decreased evoked release observed in $P[syt^{A\text{-}RQ}]$ and $P[syt^{B\text{-}RQ}]$ mutants is not the result of protein misexpression

It is conceivable that the decreased evoked release demonstrated in both the $P[syt^{A\text{-}RQ}]$ and $P[syt^{B\text{-}RQ}]$ mutants results from protein misexpression. To assess the expression level of each transgenic line, we probed Western blots of larval CNSs with an anti-synaptotagmin antibody (Fig. 4*A*) ($P[syt^{WT}]$, $P[syt^{A\text{-}RQ}]$ line 8, and $P[syt^{B\text{-}RQ}]$ line 3 shown). The two independent lines of both $P[syt^{A\text{-}RQ}]$ and $P[syt^{B\text{-}RQ}]$ used for the electrophysiological experiments expressed approximately the same amount of transgenic synaptotagmin as the transgenic control line (Fig. 4*B*). Thus, the deficits in evoked release seen in both the $P[syt^{A\text{-}RQ}]$ and $P[syt^{B\text{-}RQ}]$ mutants are not the result of insufficient expression of the transgene. To determine whether the mutant proteins were appropriately localized to synaptic sites, the neuromuscular junctions of mutant and control transgenic larvae were immunolabeled with an anti-synaptotagmin antibody. In all lines, transgenic synaptotagmin was properly localized to the neuromuscular junction (Fig. 4*C*) ($P[syt^{WT}]$, $P[syt^{A\text{-}RQ}]$ line 8, and $P[syt^{B\text{-}RQ}]$ line 4 shown). Thus, the decrease in evoked release did not result from either a deficiency in gene dosage or improper localization.

The $syt^{A\text{-}RQ}$ and $syt^{B\text{-}RQ}$ mutations decrease the Ca^{2+} affinity of neurotransmitter release

Release of neurotransmitter has long been known to be a Ca^{2+}-dependent, cooperative process (Dodge and Rahamimoff, 1967). The Ca^{2+} cooperativity ("*n*") of release may represent the mean number of Ca^{2+} ions used to trigger a vesicle fusion event (Dodge and Rahamimoff, 1967; Stevens and Sullivan, 2003; Tamura et al., 2007). To assess the Ca^{2+} dependence of the release properties in the $syt^{A\text{-}RQ}$ and $syt^{B\text{-}RQ}$ mutants, evoked release was measured at a variety of extracellular Ca^{2+} concentrations, ranging from 0.6 to 5.0 mM. At all Ca^{2+} concentrations, these mutants exhibit a decrease in evoked transmitter release compared with control (Fig. 5*A*). To determine whether mutation of either of these basic residues changes the Ca^{2+} cooperativity of release, we plotted the mean EJP amplitude versus extracellular Ca^{2+} concentration on a double-log plot in nonsaturating Ca^{2+} ranges (Fig. 5*B*). As estimated from the slope of these double-log plots, $n = 3.2$ for $P[syt^{WT}]$, $n = 3.0$ for $P[syt^{A\text{-}RQ}]$, and $n = 2.9$ for $P[syt^{B\text{-}RQ}]$, similar to previously recorded values ($n = 3.0$–3.6) at wild-type neuromuscular junctions in *Drosophila* (Littleton et al., 1994; Stewart et al., 2000; Yoshihara and Littleton, 2002; Okamoto et al., 2005). Thus, neither of the mutations changes the Ca^{2+} cooperativity of release. This finding is consistent with the hypothesis that synaptotagmin's interaction with phospholipids functions downstream of Ca^{2+} binding and does not affect the number of Ca^{2+} ions needed to trigger vesicle fusion.

To assess the apparent Ca^{2+} affinity of release, we fit the Hill equation to the data and normalized to the predicted maximal

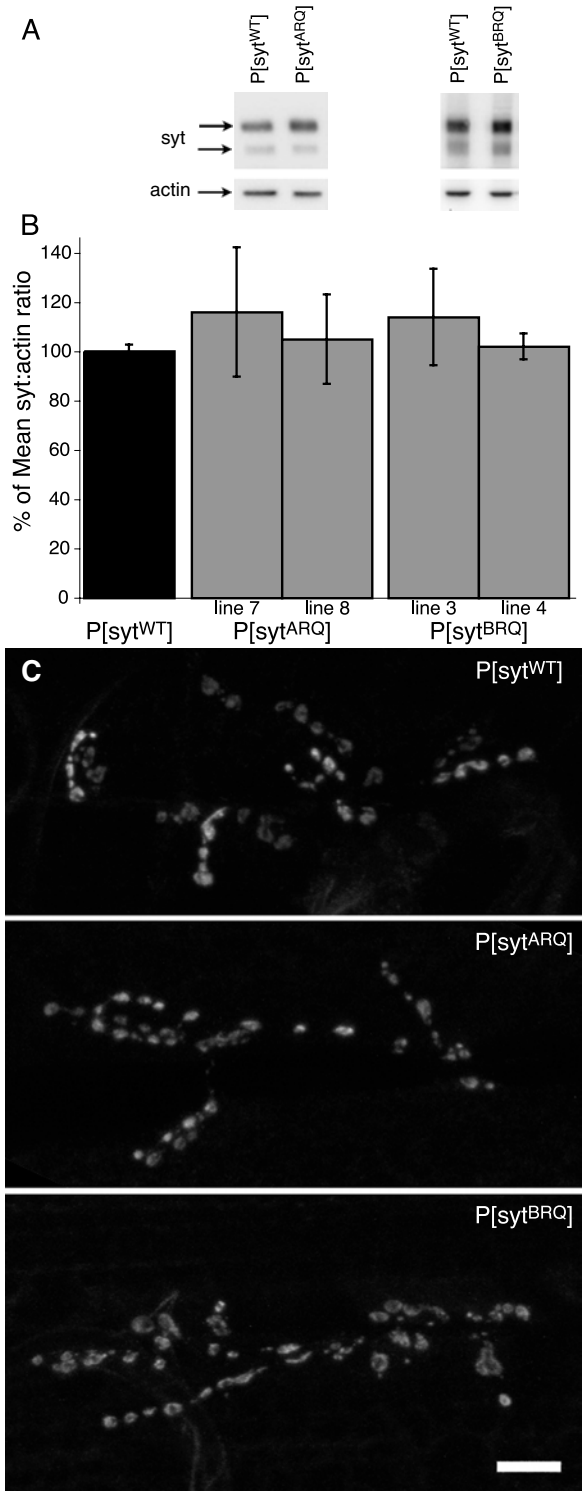

Figure 4. Synaptotagmin expression is unaltered in phospholipid-binding mutants. ***A***, Synaptotagmin is expressed at similar levels in each of the transgenic synaptotagmin lines. Representative Western blots of homogenized CNSs of third instars from the indicated lines were probed with an anti-synaptotagmin antibody. To confirm equal loading, they were also probed with an anti-actin antibody. ***B***, Comparison of synaptotagmin/actin ratio normalized to the mean ratio of the transgenic control for $P[syt^{WT}]$ ($n = 45$), $P[syt^{A\text{-}RQ}]$ line 7 ($n = 6$), $P[syt^{A\text{-}RQ}]$ line 8 ($n = 14$), $P[syt^{B\text{-}RQ}]$ line 3 ($n = 18$), and $P[syt^{B\text{-}RQ}]$ line 4 ($n = 10$). An ANOVA showed no significant difference between any of the genotypes ($p > 0.1$). ***C***, Synaptotagmin is localized to the larval neuromuscular junction in each of the transgenic synaptotagmin lines. Representative confocal *Z*-stack projections are shown for $P[syt^{WT}]$, $P[syt^{A\text{-}RQ}]$ line 8, and $P[syt^{B\text{-}RQ}]$ line 4. Scale bar, 10 μm.

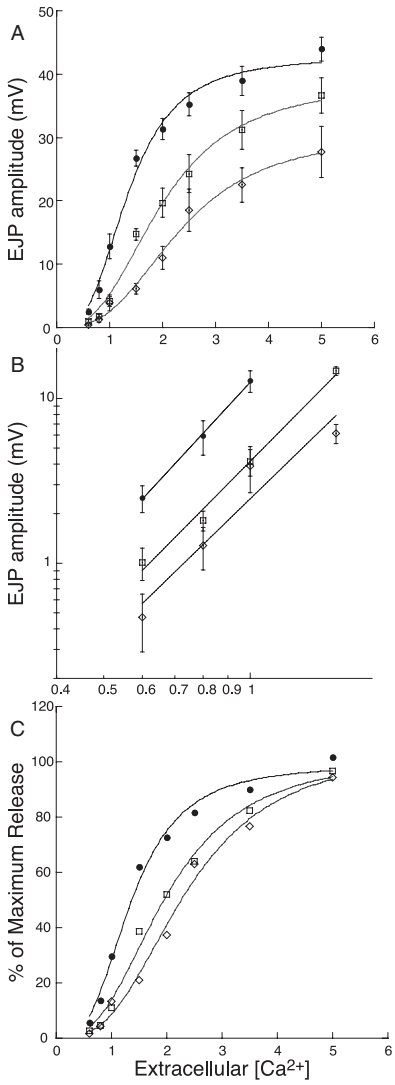

Figure 5. Phospholipid-binding mutants decrease the apparent Ca^{2+} affinity but do not affect the Ca^{2+} cooperativity of release. ***A***, EJPs were evoked in $P[syt^{WT}]$, $P[syt^{A\text{-}RQ}]$ line 8, and $P[syt^{B\text{-}RQ}]$ lines 3 and 4 by 0.05 Hz stimulation, and 10 sweeps were averaged for each fiber at each $[Ca^{2+}]$. The responses from lines 3 and 4 of $P[syt^{B\text{-}RQ}]$ were not significantly different, so the results were pooled. For all genotypes at all $[Ca^{2+}]$, $n = 10–18$ muscle fibers, except for 1.5 mM Ca^{2+}, at which $n = 40–49$ muscle fibers. The Hill equation was fit to the data. Error bars are SEM. ***B***, The EJP amplitudes within the nonsaturating range of Ca^{2+} were plotted on a double-log plot, and a linear regression line was used to determine the slope (*n*) ($P[syt^{WT}]$: $n = 3.2$, $r = 0.999$; $P[syt^{A\text{-}RQ}]$: $n = 3.0$, $r = 0.999$; $P[syt^{B\text{-}RQ}]$: $n = 2.9$, $r = 0.933$). ***C***, The EJP amplitudes at each Ca^{2+} concentration were normalized to the maximum predicted by the Hill equation for each genotype and replotted to illustrate the shift in EC_{50}. $P[syt^{WT}]$: $EC_{50} = 1.4 \pm 0.1$ mM; $P[syt^{A\text{-}RQ}]$: $EC_{50} = 2.0 \pm 0.1$ mM; $P[syt^{B\text{-}RQ}]$: $EC_{50} = 2.3 \pm 0.2$ mM. For all panels, black filled circles indicate $P[syt^{WT}]$, gray open squares indicate $P[syt^{A\text{-}RQ}]$, and gray open diamonds indicate $P[syt^{B\text{-}RQ}]$.

response within each line. Figure 5*C* shows that the apparent Ca^{2+} affinity of release *in vivo* was decreased in both the $P[syt^{A\text{-}RQ}]$ ($EC_{50} = 2.0 \pm 0.1$ mM) and $P[syt^{B\text{-}RQ}]$ ($EC_{50} = 2.3 \pm 0.2$ mM) mutants compared with the transgenic wild-type control ($EC_{50} = 1.4 \pm 0.1$ mM). A rightward shift of the EC_{50} for Ca^{2+}-evoked transmitter release was previously seen for $syt^{A\text{-}RQ}$ mutants in several cell culture systems, including hippocampal autapses, chromaffin cells, and PC12 cells (Fernández-Chacón et al., 2001; Sørensen et al., 2003; Wang et al., 2003), and our studies now show that the $syt^{A\text{-}RQ}$ mutation decreases the Ca^{2+} affinity of release at an intact synapse. In addition, our experiments dem-

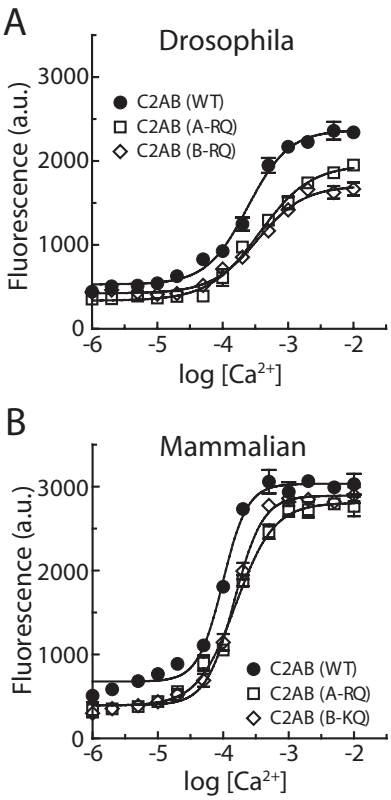

Figure 6. Mutation of the conserved basic residue in either C_2A or C_2B decreases Ca^{2+}-dependent interactions between anionic phospholipids and synaptotagmin in both *Drosophila* and mammals. Phospholipid binding for wild-type (black filled circles), C_2A mutant (gray open squares; A-RQ in both *Drosophila* and mammals), and C_2B mutant (gray open diamonds; B-RQ in *Drosophila* and B-KQ in mammals) C_2AB domains are graphed versus Ca^{2+} concentration. ***A***, Immobilized WT or A-RQ or B-RQ mutant versions of *Drosophila* C_2AB were assayed for binding PS/PC liposomes. The A-RQ and the B-RQ mutations each decreased the apparent Ca^{2+} affinity of binding by ~1.5-fold compared with WT without altering the Hill coefficient. The EC_{50} (mean ± SD in micromolar concentration) was 368 ± 35 for A-RQ, 344 ± 32 for B-RQ, and 238 ± 20 for WT. ***B***, Immobilized WT, A-RQ, or B-KQ mutant versions of mammalian C_2AB were assayed for binding PS/PC liposomes. The A-RQ and the B-KQ mutations each decreased the apparent Ca^{2+} affinity of binding by ~1.5-fold compared with WT without altering the Hill coefficient. The EC_{50} (mean ± SD in micromolar concentration) was 154 ± 10 for A-RQ, 147 ± 7 for B-KQ, and 98 ± 6 for WT.

onstrate that the $syt^{B\text{-}RQ}$ mutation also results in a severe disruption of Ca^{2+}-evoked transmitter release at an intact synapse, indicating that the function of the basic residue at the tip of loop 3 is conserved.

The $syt^{A\text{-}RQ}$ and $syt^{B\text{-}RQ}$ mutations decrease the Ca^{2+} affinity of phospholipid binding

To determine whether the conserved basic residue at the tip of each C_2 domain participates in the electrostatic interaction between synaptotagmin and anionic phospholipids, we measured the Ca^{2+} affinity of C_2AB domain binding to PS/PC liposomes *in vitro*. Similar to previous reports from mammalian systems (Chae et al., 1998; Davletov et al., 1998; Fernandez et al., 2001; Fernández-Chacón et al., 2001; Wang et al., 2003), the *Drosophila* $syt^{A\text{-}RQ}$ mutation decreased the Ca^{2+} affinity of C_2AB binding to negatively charged phospholipids (Fig. 6*A*) (WT EC_{50} = 238 ± 20 μM Ca^{2+}; $syt^{A\text{-}RQ}$ EC_{50} = 368 ± 35 μM Ca^{2+}). Using *Drosophila* C_2AB domains, the $syt^{B\text{-}RQ}$ mutation decreased the Ca^{2+} affinity of binding to negatively charged phospholipids to a similar extent as the $syt^{A\text{-}RQ}$ mutation (Fig. 6*A*) (WT EC_{50} = 238 ± 20 μM Ca^{2+}; $syt^{B\text{-}RQ}$ EC_{50} = 344 ± 32 μM Ca^{2+}). Compared with mammalian systems, this result is consistent with the findings of Wang et al. (2003) but in conflict with the findings of Li et al. (2006). To directly examine whether or not the *Drosophila* and mammalian systems differ, we also measured the Ca^{2+} affinity of mammalian C_2AB domain binding to PS/PC liposomes. As shown in Figure 6*B*, both the $syt^{A\text{-}RQ}$ and the $syt^{B\text{-}KQ}$ mutations decreased the Ca^{2+} affinity of C_2AB binding to negatively charged phospholipids to a similar extent (WT EC_{50} = 98 ± 6 μM Ca^{2+}; $syt^{A\text{-}RQ}$ EC_{50} = 154 ± 10 μM Ca^{2+}; $syt^{B\text{-}KQ}$ EC_{50} = 147 ± 7 μM Ca^{2+}). The EC_{50} values measured in this study are higher than those previously reported (Fernández-Chacón et al., 2001; Wang et al., 2003) because of a lower, and more physiological (Takamori et al., 2006), percentage of negatively charged phospholipids in our liposomes. Thus, in *Drosophila* and mammals, mutation of either the C_2A or the C_2B conserved basic residue decreases the Ca^{2+} affinity of interactions with anionic phospholipids.

Discussion

Several reports indicate that residues at the tip of the Ca^{2+}-binding pockets, including the conserved basic residues, in both C_2 domains of synaptotagmin are critical for Ca^{2+}-dependent phospholipid interactions *in vitro* and Ca^{2+}-triggered fusion in cultured cells (Chapman and Davis, 1998; Fernández-Chacón et al., 2001; Bai et al., 2002; Frazier et al., 2003; Sørensen et al., 2003; Wang et al., 2003; Rhee et al., 2005; Araç et al., 2006). Studying cultured cells provides valuable insight into possible protein functions, yet some of the properties of vesicle fusion in PC12 cells and chromaffin cells are quite different from those mediating fast transmitter release at a synapse. Even cultured neurons do not necessarily faithfully reproduce all aspects of synaptic behavior at an intact synapse. For example, at cultured hippocampal autapses, the amplitude of mEJPs is larger (Bekkers et al., 1990), the paired-pulse ratio is decreased (Sippy et al., 2003), and long-term potentiation cannot be reliably elicited (Bekkers and Stevens, 1990) compared with recordings from hippocampal slices. Additionally, synaptotagmin mutant autapses exhibit no change in mEJP frequency (Geppert et al., 1994), whereas synaptotagmin mutations increased the mEJP frequency at several other synapses, including excitatory and inhibitory synapses between cultured cortical neurons, the calyx of Held, and mature neuromuscular junctions in *Drosophila* and mice (DiAntonio and Schwarz, 1994; Pang et al., 2006a,c) (but see Marek and Davis, 2002). Therefore, it is critical to test the function of the basic residues at the tips of the C_2 domains at an intact synapse to determine their role in synaptic transmission *in vivo*.

The C_2A and C_2B domains are structurally highly homologous and exhibit many similar biochemical interactions *in vitro* (Geppert et al., 1991; Sutton et al., 1995; Chae et al., 1998; Shao et al., 1998; Ubach et al., 1998; Fernandez et al., 2001; Cheng et al., 2004). Analyses of these interactions have provided critical insights into the molecular mechanisms mediating synaptic vesicle fusion. Conditions *in vitro*, however, can affect biochemical interactions. Interactions between the C_2A basic residue and negatively charged phospholipids can differ when isolated C_2A domains are used: Fernández-Chacón et al. (2001) found that the Ca^{2+} affinity of the interaction was decreased in $syt^{A\text{-}RQ}$ mutants, whereas Zhang et al. (1998) found no change. But studies using tandem C_2AB domains all show a decrease in Ca^{2+}-dependent phospholipid binding (Fernández-Chacón et al., 2001; Wang et al., 2003; Li et al., 2006). The homologous C_2B residue shows variable results using tandem C_2AB domains: similar to our re-

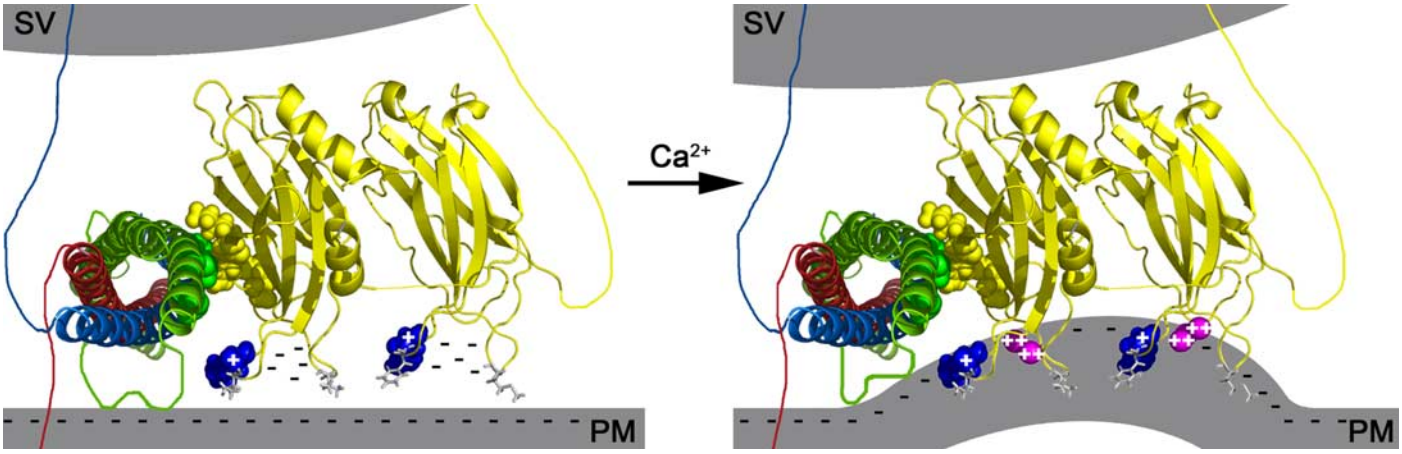

Figure 7. Model of the role played by the conserved basic residues in Ca^{2+}-dependent interactions with the anionic presynaptic membrane. The crystal structure of the core complex [PDB file 1SFC, containing syntaxin (red), SNAP-25 (green), and VAMP (vesicle-associated membrane protein)/synaptobrevin (blue)], the nuclear magnetic resonance structures of the C_2A (PDB file 1BYN) and C_2B (PDB file 1K5W) domains of synaptotagmin (yellow), and Ca^{2+} (pink) are shown to scale using PyMOL Molecular Graphics System (DeLano Scientific). The membranes, the transmembrane domains, and the link between C_2A and C_2B were added in Adobe Photoshop. Left, A Ca^{2+}-independent priming interaction between the C_2B polylysine motif (yellow, space-filled residues) and SNAP-25 (green, space-filled residues) holds the C_2A and C_2B Ca^{2+} binding sites in close proximity to the presynaptic membrane. We diagrammed the interaction between the C_2B polylysine motif and SNAP-25 within the SNARE complex (Zhang et al., 2002; Rickman et al., 2004, 2006; Dai et al., 2007), because mutation of the C_2B polylysine motif impairs this interaction (Bai et al., 2004) and disrupts synaptotagmin's ability to increase the speed of SNARE-mediated liposome fusion in the absence of any PIP_2 (Loewen et al., 2006). However, an interaction with PIP_2, which is located specifically in the presynaptic membrane, could also serve this purpose (Bai et al., 2004; Araç et al., 2006). In the absence of Ca^{2+}, the high concentration of negative charge in the Ca^{2+}-binding pockets repulses the negatively charged presynaptic membrane, preventing synaptotagmin's conserved basic residues (blue, space-filled residues) from interacting with the membrane. Right, After Ca^{2+} entry, the negative charge of the Ca^{2+}-binding pockets is neutralized by the bound Ca^{2+}, which initiates the electrostatic switch: a strong attraction of the negatively charged, phospholipid head groups by the bound Ca^{2+} and the basic residues at the tips of Ca^{2+}-binding pockets that draws the synaptic vesicle (SV) toward the presynaptic membrane (PM). Insertion of the hydrophobic residues (gray, stick residues) at the tips of the C_2 domains into the core of the presynaptic membrane (Chapman and Davis, 1998) may help trigger fusion by promoting a local Ca^{2+}-dependent buckling of the plasma membrane (Chapman and Davis, 1998; Martens et al., 2007). The Ca^{2+}-induced increase in positive charge at the end of the C_2B domain also likely increases the strength of the electrostatic interaction between the C_2B polylysine motif and the SNARE complex, resulting in simultaneous binding of the SNARE complex and the presynaptic membrane (Davis et al., 1999; Bhalla et al., 2006; Loewen et al., 2006; Dai et al., 2007).

sults in *Drosophila* (Fig. 6*A*), Wang et al. (2003) found that this mutation decreased Ca^{2+}-dependent interactions with negatively charged phospholipids, whereas Li et al. (2006) found no change. We therefore repeated these experiments using the C_2AB constructs from Li et al. (2006) and found that the Ca^{2+} affinity of this interaction decreased (Fig. 6*B*). Thus, Ca^{2+}-dependent interactions between these positively charged residues and negatively charged phospholipids appear to be quite sensitive to experimental conditions. Still, most studies find a decrease in Ca^{2+}-dependent phospholipid interactions when either the C_2A or C_2B basic residue is neutralized.

Additional studies indicate that Ca^{2+}-dependent interactions between each C_2 domain and anionic membranes are conserved and mediated by residues at the tip of the Ca^{2+}-binding pockets. Immediately adjacent to the conserved basic residues (Fig. 1, ⊕), there are hydrophobic residues (Fig. 1*A*, □). In both C_2 domains, these hydrophobic residues interact with phospholipids in a Ca^{2+}-dependent manner by inserting into the hydrophobic core of the membrane (Bai et al., 2002). Increasing the hydrophobicity of three residues located around the rim of each Ca^{2+}-binding pocket substantially increased the Ca^{2+} affinity of these interactions (Rhee et al., 2005). Together, these results provide strong support for the hypothesis that Ca^{2+}-dependent interactions between phospholipids and both the C_2A and C_2B domains are mediated by residues located at the tip of the Ca^{2+}-binding pockets.

But are these interactions between synaptotagmin and anionic membranes relevant for synaptic transmission? Results from cultured cells suggest that residues at the tip of the C_2A Ca^{2+}-binding pocket maybe functionally significant; the $syt^{A\text{-}RQ}$ mutation decreased evoked transmitter release by decreasing the apparent Ca^{2+} affinity of release (Fernández-Chacón et al., 2001; Sørensen et al., 2003; Wang et al., 2003). The homologous mutation in C_2B has been examined twice in culture with directly contradictory results. At cultured hippocampal autapses, this mutation showed no decrease in Ca^{2+}-evoked release (Li et al., 2006). However, in cultured PC12 cells, the C_2B mutation decreased Ca^{2+}-evoked release (Wang et al., 2003). Thus, the functional relevance of the C_2B interaction remained inconclusive.

To determine whether the results from cultured cells are relevant for synaptic transmission *in vivo*, we tested the function of the basic residue at the tip of each Ca^{2+}-binding pocket at intact neuromuscular junctions. We found that the $syt^{A\text{-}RQ}$ mutation decreases the Ca^{2+} affinity of release at the neuromuscular junction. Importantly, we found that the $syt^{B\text{-}RQ}$ mutation also decreases Ca^{2+}-evoked transmitter release by decreasing Ca^{2+} affinity. Western analysis and immunohistochemical localization studies demonstrate approximately equal levels of transgene expression and appropriate synaptic localization in multiple, independent mutant and control lines. Therefore the decrease in evoked release is a direct result of the mutation. Thus, both the C_2A and C_2B positively charged residues mediate Ca^{2+}-dependent interactions with anionic phospholipids and are required for efficient evoked transmitter release at intact synapses.

Our results are consistent with those from PC12 cells expressing the mutant C_2B protein (Wang et al., 2003). When using high K^+ to trigger release, these authors found that the rate of evoked release was decreased by ~50% in both the C_2A and C_2B basic residue mutations. Interestingly, the cumulative amount of release was lower in C_2B mutants than in C_2A mutants, although this effect was not quantified. Yet our results at intact synapses, like the results from PC12 cells, are in direct contrast with the lack of effect seen at hippocampal autapses (Li et al., 2006).

Importantly, the replacement of three hydrophobic residues

around the rim of either the C_2A or the C_2B Ca^{2+}-binding pocket with residues of increased hydrophobicity increased both the Ca^{2+} affinity of phospholipid binding *in vitro* and the Ca^{2+} affinity of evoked release at autapses (Rhee et al., 2005). Thus, even at hippocampal autapses, the tip of the C_2B Ca^{2+}-binding pocket can interact with phospholipid membranes during synaptic transmission.

Our results indicate that the function of this basic residue is conserved in each C_2 domain. Yet other studies have discovered dramatic functional differences between the C_2 domains during synaptic transmission. The most striking difference is the relative importance of Ca^{2+} binding in triggering vesicle fusion. Mutations within the C_2A Ca^{2+}-binding motif resulted in either subtle or no disruptions in evoked release (Fernández-Chacón et al., 2002; Robinson et al., 2002; Stevens and Sullivan, 2003; Pang et al., 2006b). Yet mutations within the C_2B Ca^{2+}-binding motif inhibited evoked release by up to 99% (Mackler and Reist, 2001; Nishiki and Augustine, 2004; Tamura et al., 2007). Thus, Ca^{2+} binding by the C_2B domain plays the crucial role in triggering fast, synchronous vesicle fusion.

The key difference between the C_2 domains likely resides within their polylysine motifs. The C_2B polylysine motif mediates a unique set of interactions that are not shared by the C_2A domain, including Ca^{2+}-independent interactions with phosphatidylinositol 4,5-bisphosphate (PIP_2) and soluble *N*-ethylmaleimide-sensitive factor attachment receptor (SNARE) proteins (Zhang et al., 2002; Bai et al., 2004; Rickman et al., 2004). Because the polylysine motif is on the side of the C_2B domain, interactions with the SNARE proteins could hold the C_2B Ca^{2+}-binding pocket in close proximity to the presynaptic membrane, priming vesicles for immediate fusion after Ca^{2+} influx (Fig. 7*A*) (Loewen et al., 2006). Then, after Ca^{2+} influx, the conserved basic residues of each C_2 domain mediate similar Ca^{2+}-dependent interactions with anionic phospholipids (Fig. 6) (Wang et al., 2003), which pulls the synaptic vesicle toward the membrane (Fig. 7*B*). The insertion of hydrophobic residues on the tips of the C_2 domains may destabilize the presynaptic membrane, aiding the fusion reaction (Bai et al., 2002; Martens et al., 2007). The relative positioning of the C_2A versus C_2B domains with respect to the SNARE complex may determine the relative importance of the Ca^{2+}-binding sites, and the basic residues reported in this study, for triggering vesicle fusion *in vivo*. This model is consistent with the data from multiple *in vitro* and *in vivo* systems, and a remarkably similar model, postulating a more distally positioned C_2A domain, has recently been proposed (Dai et al., 2007).

In summary, synchronous vesicle fusion triggered by Ca^{2+} requires the coordinated interactions of many presynaptic molecules. Examination of isolated interactions *in vitro* provides insight into possible molecular mechanisms for fusion; however, only the analysis of synaptic transmission at intact synapses can determine which interactions are likely to function *in vivo*. Our findings demonstrate that the positively charged residue located at the tip of each Ca^{2+}-binding pocket mediates Ca^{2+}-dependent interactions with negatively charged membranes and is required for efficient synaptic transmission. These findings indicate that the function of this region of C_2A and C_2B is likely conserved and support the hypothesis that Ca^{2+}-dependent interactions between the tips of each C_2 domain with anionic phospholipids are requisite for efficient excitation–secretion coupling during synaptic transmission.

References

Araç D, Chen X, Khant HA, Ubach J, Ludtke SJ, Kikkawa M, Johnson AE, Chiu W, Südhof TC, Rizo J (2006) Close membrane-membrane proximity induced by Ca(2+)-dependent multivalent binding of synaptotagmin-1 to phospholipids. Nat Struct Mol Biol 13:209–217.

Bai J, Wang P, Chapman ER (2002) C2A activates a cryptic Ca(2+)-triggered membrane penetration activity within the C2B domain of synaptotagmin I. Proc Natl Acad Sci U S A 99:1665–1670.

Bai J, Tucker WC, Chapman ER (2004) PIP2 increases the speed of response of synaptotagmin and steers its membrane-penetration activity toward the plasma membrane. Nat Struct Mol Biol 11:36–44.

Banker G, Goslin K, eds (1998) Culturing nerve cells, Ed 2. Cambridge, MA: MIT.

Bekkers JM, Stevens CF (1990) Presynaptic mechanism for long-term potentiation in the hippocampus. Nature 346:724–729.

Bekkers JM, Richerson GB, Stevens CF (1990) Origin of variability in quantal size in cultured hippocampal neurons and hippocampal slices. Proc Natl Acad Sci U S A 87:5359–5362.

Bhalla A, Chicka MC, Tucker WC, Chapman ER (2006) Ca2+-synaptotagmin directly regulates t-SNARE function during reconstituted membrane fusion. Nat Struct Mol Biol 13:323–330.

Brand AH, Perrimon N (1993) Targeted gene expression as a means of altering cell fates and generating dominant phenotypes. Development 118:401–415.

Chae YK, Abildgaard F, Chapman ER, Markley JL (1998) Lipid binding ridge on loops 2 and 3 of the C2A domain of synaptotagmin I as revealed by NMR spectroscopy. J Biol Chem 273:25659–25663.

Chapman ER, Davis AF (1998) Direct interaction of a Ca2+-binding loop of synaptotagmin with lipid bilayers. J Biol Chem 273:13995–14001.

Chapman ER, Hanson PI, An S, Jahn R (1995) Ca2+ regulates the interaction between synaptotagmin and syntaxin I. J Biol Chem 270:23667–23671.

Cheng Y, Sequeira SM, Malinina L, Tereshko V, Söllner TH, Patel DJ (2004) Crystallographic identification of Ca2+ and Sr2+ coordination sites in synaptotagmin I C2B domain. Protein Sci 13:2665–2672.

Dai H, Shen N, Araç D, Rizo J (2007) A quaternary SNARE-synaptotagmin-Ca2+-phospholipid complex in neurotransmitter release. J Mol Biol 367:848–863.

Davis AF, Bai J, Fasshauer D, Wolowick MJ, Lewis JL, Chapman ER (1999) Kinetics of synaptotagmin responses to Ca2+ and assembly with the core SNARE complex into membranes. Neuron 24:363–376.

Davletov B, Perisic O, Williams RL (1998) Calcium-dependent membrane penetration is a hallmark of the C2 domain of cytosolic phospholipase A2 whereas the C2A domain binds membranes electrostatically. J Biol Chem 273:19093–19096.

DiAntonio A, Schwarz TL (1994) The effect on synaptic physiology of synaptotagmin mutations in *Drosophila*. Neuron 12:909–920.

Dodge FA Jr, Rahamimoff R (1967) Co-operative action a calcium ions in transmitter release at the neuromuscular junction. J Physiol 193:419–432.

Earles CA, Bai J, Wang P, Chapman ER (2001) The tandem C2 domains of synaptotagmin contain redundant Ca2+ binding sites that cooperate to engage t-SNAREs and trigger exocytosis. J Cell Biol 154:1117–1123.

Fernandez I, Araç D, Ubach J, Gerber SH, Shin O, Gao Y, Anderson RG, Südhof TC, Rizo J (2001) Three-dimensional structure of the synaptotagmin 1 C2B-domain: synaptotagmin 1 as a phospholipid binding machine. Neuron 32:1057–1069.

Fernández-Chacón R, Königstorfer A, Gerber SH, García J, Matos MF, Stevens CF, Brose N, Rizo J, Rosenmund C, Südhof TC (2001) Synaptotagmin I functions as a calcium regulator of release probability. Nature 410:41–49.

Fernández-Chacón R, Shin O-H, Königstorfer A, Matos MF, Meyer AC, Garcia J, Gerber SH, Rizo J, Südhof TC, Rosenmund C (2002) Structure/function analysis of Ca2+ binding to the C2A domain of synaptotagmin I. J Neurosci 22:8438–8446.

Frazier AA, Roller CR, Havelka JJ, Hinderliter A, Cafiso DS (2003) Membrane-bound orientation and position of synaptotagmin I C2A domain by site-directed spin labeling. Biochemistry 42:96–105.

Geppert M, Archer BT 3rd, Südhof TC (1991) Synaptotagmin II: a novel differentially distributed form of synaptotagmin. J Biol Chem 266:13548–13552.

Geppert M, Goda Y, Hammer RE, Li C, Rosahl TW, Stevens CF, Südhof TC

(1994) Synaptotagmin I: a major Ca2+ sensor for transmitter release at a central synapse. Cell 79:717–727.

Han W, Rhee JS, Maximov A, Lao Y, Mashimo T, Rosenmund C, Südhof TC (2004) N-Glycosylation is essential for vesicular targeting of synaptotagmin I. Neuron 41:85–99.

Hui E, Bai J, Wang P, Sugimori M, Llinas RR, Chapman ER (2005) Three distinct kinetic groupings of the synaptotagmin family: candidate sensors for rapid and delayed exocytosis. Proc Natl Acad Sci U S A 102:5210–5214.

Li L, Shin OH, Rhee JS, Araç D, Rah JC, Rizo J, Südhof T, Rosenmund C (2006) Phosphotidylinositol phosphates as co-activators of Ca2+ binding to C2 domains of synaptotagmin I. J Biol Chem 281:15845–15852.

Littleton JT, Stern M, Perin M, Bellen HJ (1994) Calcium dependence of neurotransmitter release and rate of spontaneous vesicle fusions are altered in *Drosophila* synaptotagmin mutants. Proc Natl Acad Sci U S A 91:10888–10892.

Loewen CA, Mackler JM, Reist NE (2001) *Drosophila* synaptotagmin I null mutants survive to early adulthood. Genesis 31:30–36.

Loewen CA, Lee S-M, Shin Y-K, Reist NE (2006) C2B polylysine motif of synaptotagmin facilitates a Ca2+-independent stage of synaptic vesicle priming in vivo. Mol Biol Cell 17:5211–5226.

Mackler JM, Reist NE (2001) Mutations in the second C2 domain of synaptotagmin disrupt synaptic transmission at *Drosophila* neuromuscular junctions. J Comp Neurol 436:4–16.

Mackler JM, Drummond JA, Loewen CA, Robinson IM, Reist NE (2002) The C(2)B Ca(2+)-binding motif of synaptotagmin is required for synaptic transmission in vivo. Nature 418:340–344.

Marek KW, Davis GW (2002) Transgenically encoded protein photoinactivation (FlAsH-FALI): acute inactivation of synaptotagmin I. Neuron 36:805–813.

Martens S, Kozlov MM, McMahon HT (2007) How synaptotagmin promotes membrane fusion. Science 316:1205–1208.

Micheva KD, Holz RW, Smith SJ (2001) Regulation of presynaptic phosphatidylinositol 4,5-bisphosphate by neuronal activity. J Cell Biol 154:355–368.

Nishiki T, Augustine GJ (2004) Dual roles of the C2B domain of synaptotagmin I in synchronizing Ca^{2+}-dependent neurotransmitter release. J Neurosci 24:8542–8550.

Okamoto T, Tamura T, Suzuki K, Kidokoro Y (2005) External Ca2+ dependency of synaptic transmission in *Drosophila* synaptotagmin I mutants. J Neurophysiol 2005:1574–1586.

Pang ZP, Sun J, Rizo J, Maximov A, Südhof TC (2006a) Genetic analysis of synaptotagmin 2 in spontaneous and Ca2+ triggered neurotransmitter release. EMBO J 25:2039–2050.

Pang ZP, Shin OH, Meyer AC, Rosenmund C, Südhof TC (2006b) A gain of function mutant in synaptotagmin I reveals a critical role of Ca^{2+}-dependent soluble *N*-ethylmaleimide-sensitive factor attachment protein receptor complex binding in synaptic exocytosis. J Neurosci 26:12556–12565.

Pang ZP, Melicoff E, Padgett D, Liu Y, Teich AF, Dickey BF, Lin W, Adachi R, Südhof TC (2006c) Synaptotagmin-2 is essential for survival and contributes to Ca^{2+} triggering of neurotransmitter release in central and neuromuscular synapses. J Neurosci 26:13493–13504.

Perin MS, Fried VA, Mignery GA, Jahn R, Südhof TC (1990) Phospholipid binding by a synaptic vesicle protein homologous to the regulatory region of protein kinase C. Nature 345:260–263.

Rhee JS, Li LY, Shin OH, Rah JC, Rizo J, Südhof TC, Rosenmund C (2005) Augmenting neurotransmitter release by enhancing the apparent Ca2+ affinity of synaptotagmin I. Proc Natl Acad Sci U S A 102:18664–18669.

Rickman C, Meunier FA, Binz T, Davletov B (2004) High affinity interaction of syntaxin and SNAP-25 on the plasma membrane is abolished by botulinum toxin E. J Biol Chem 279:644–651.

Rickman C, Jiménez JL, Graham ME, Archer DA, Soloviev M, Burgoyne RD, Davletov B (2006) Conserved prefusion protein assembly in regulated exocytosis. Mol Biol Cell 17:283–294.

Robinson IM, Ranjan R, Schwarz TL (2002) Synaptotagmins I and IV promote transmitter release independently of Ca(2+) binding in the C(2)A domain. Nature 418:336–340.

Shao X, Fernandez I, Südhof TC, Rizo J (1998) Solution structures of the Ca2+-free and Ca2+-bound C2A domain of synaptotagmin I: does Ca2+ induce a conformational change? Biochemistry 37:16106–16115.

Sippy T, Cruz-Martín A, Jeromin A, Schweizer FE (2003) Acute changes in short-term plasticity at synapses with elevated levels of neuronal calcium sensor-1. Nat Neurosci 6:1031–1038.

Sørensen JB, Fernández-Chacón R, Südhof TC, Neher E (2003) Examining synaptotagmin 1 function in dense core vesicle exocytosis under direct control of Ca2+. J Gen Physiol 122:265–276.

Stevens CF, Sullivan JM (2003) The synaptotagmin C2A domain is part of the calcium sensor controlling fast synaptic transmission. Neuron 39:299–308.

Stewart BA, Atwood HL, Renger JJ, Wang J, Wu CF (1994) Improved stability of *Drosophila* larval neuromuscular preparations in haemolymph-like physiological solutions. J Comp Physiol [A] 175:179–191.

Stewart BA, Mohtashami M, Trimble WS, Boulianne GL (2000) SNARE proteins contribute to the calcium cooperativity of synaptic transmission. Proc Natl Acad Sci U S A 97:13955–13960.

Sutton RB, Davletov BA, Berghuis AM, Südhof TC, Sprang SR (1995) Structure of the first C2 domain of synaptotagmin I: A novel Ca2+/phospholipid binding fold. Cell 80:929–938.

Takamori S, Holt M, Stenius K, Lemke EA, Grønborg M, Riedel D, Urlaub H, Schenck S, Brügger B, Ringler P, Müller SA, Rammner B, Gräter F, Hub JS, De Groot BL, Mieskes G, Moriyama Y, Klingauf J, Grubmüller H, Heuser J, et al. (2006) Molecular anatomy of a trafficking organelle. Cell 127:831–846.

Tamura T, Hou J, Reist NE, Kidokoro Y (2007) Nerve-evoked synchronous release and high K+-induced quantal events are regulated separately by synaptotagmin I at *Drosophila* neuromuscular junctions. J Neurophysiol 97:540–549.

Ubach J, Zhang X, Shao X, Südhof TC, Rizo J (1998) Ca2+ binding to synaptotagmin: how many Ca2+ ions bind to the tip of a C2-domain? EMBO J 17:3921–3930.

Ubach J, Lao Y, Fernandez I, Arac D, Südhof TC, Rizo J (2001) The C2B domain of synaptotagmin I is a Ca2+-binding module. Biochemistry 40:5854–5860.

Wang P, Wang CT, Bai J, Jackson MB, Chapman ER (2003) Mutations in the effector binding loops in the C2A and C2B domains of synaptotagmin I disrupt exocytosis in a nonadditive manner. J Biol Chem 278:47030–47037.

Yao KM, White K (1994) Neural specificity of elav expression: defining a *Drosophila* promoter for directing expression to the nervous system. J Neurochem 63:41–51.

Yoshihara M, Littleton JT (2002) Synaptotagmin I functions as a calcium sensor to synchronize neurotransmitter release. Neuron 36:897–908.

Zhang X, Rizo J, Südhof TC (1998) Mechanism of phospholipid binding by the C2A-domain of synaptotagmin I. Biochemistry 37:12395–12403.

Zhang X, Kim-Miller MJ, Fukuda M, Kowalchyk JA, Martin TF (2002) Ca2+-dependent synaptotagmin binding to SNAP-25 is essential for Ca2+-triggered exocytosis. Neuron 34:599–611.